LAWRENCE
LIVERMORE
NATIONAL
LABORATORY

UCRL-TR-221292

Contact Interface Verification for DYNA3D

Scenario 2: Multi-Surface Contact

Larry D. McMichael

March 31, 2006

This work was performed under the auspices of the U.S. Department of Energy by University of California, Lawrence Livermore National Laboratory under Contract W-7405-Eng-48.

TABLE OF CONTENTS

Contact Interface Verification for DYNA3D
Scenario 2: Multi-Surface Contact

Larry D. McMichael
Defense Systems Analysis Group
New Technologies Engineering Division

1 INTRODUCTION

A suite of test problems has been developed to examine contact behavior within the nonlinear, three-dimensional, explicit finite element analysis (FEA) code DYNA3D (Lin, 2005). The test problems use multiple interfaces and a combination of enforcement methods to assess the basic functionality of the contact algorithms. The results from the DYNA3D analyses are compared to closed form solutions to verify the contact behavior. This work was performed as part of the Verification and Validation efforts of LLNL W Program within the NNSA's Advanced Simulation and Computing (ASC) Program.

DYNA3D models the transient dynamic response of solids and structures including the interactions between disjoint bodies (parts). A wide variety of contact surfaces are available to represent the diverse interactions possible during an analysis, including relative motion (sliding), separation and gap closure (voids), and fixed relative position (tied). The problem geometry may be defined using a combination of element formulations, including one-dimensional beam and truss elements, two-dimensional shell elements, and three-dimensional solid elements. Consequently, it is necessary to consider various element interactions during contact.

This report and associated test problems examine the scenario where multiple bodies interact with each other via multiple interfaces. The test problems focus on whether any ordering issues exist in the contact logic by using a combination of interface types, contact enforcement options (i.e., penalty, Lagrange, and kinematic), and element interactions within each problem. The influence of rigid materials on interface behavior is also examined. The companion report (McMichael, 2006) and associated test problems address the basic contact scenario where one contact surface exists between two disjoint bodies.

The test problems are analyzed using version 5.2 (compiled on 12/22/2005) of DYNA3D. The analytical results are used to form baseline solutions for subsequent regression testing.

In section 2, the test problems are presented, and the static solution is developed for two idealized systems. Section 3 describes the finite element representation of the generic problem, including the interface combinations considered. The verification criteria and expected results are presented next in section 4. Section 5 discusses the numerical results obtained from each test problem. Finally, section 6 summarizes the observed interface behavior.

2 MULTI-CONTACT PROBLEMS

Two idealized systems are developed to examine contact behavior when multiple interface types and enforcement options are present in the same problem. The first system is the simple, two-body configuration developed for the basic contact problem. However, unlike the basic contact problem, each body pair has a different interface type or enforcement algorithm. The second system is a three-body configuration that requires interaction between the contact surfaces. A quasi-static mechanics solution is developed for each system.

2.1 TWO-BODY CONTACT PROBLEM

The generic, two-body contact problem is described in detail by McMichael (2006) and will therefore only be summarized in this report. The idealized system is depicted schematically in Figure 1 with applied forces P_x and P_y. The lower block's base and right side (i.e., positive x-face) are constrained. The idealized frictional interface between the upper and lower blocks prevents relative normal displacements and allows relative tangential displacements according to a traditional Coulomb friction model. The maximum static friction force, f_s, is given by the product of the normal force, N, and the coefficient of static friction, μ_s, ($f_s = \mu_s$ N). The dynamic friction force, f_k, is given by the product of the normal force and the coefficient of kinetic friction, μ_k ($f_k = \mu_k$ N). A quasi-static solution for the interface and reaction forces is obtained by ignoring inertia effects and applying static equilibrium considerations.

Since there is no applied load in the z-direction, the interface and reaction forces in the z-direction are zero. On the upper block, the interface normal force, F_y, is equal in magnitude to the prescribed force P_y, but acts in the opposite direction. This means that the normal force controlling the available friction force is also equal to P_y (N = P_y). The interface tangential force F_x acts equal and opposite to P_x until f_s is exceeded, at which point relative motion is induced and F_x is equal to f_k. On the lower block, the reaction force in the y-direction, R_y, is equal in magnitude and direction to F_y and, therefore, also equal to P_y. The reaction force in the x-direction, R_x, is equal in magnitude and direction to F_x.

2.1.1 Theoretical Solution for Two-Body Contact

Consider the pseudo-static response to the applied loads shown in Figure 2 when $\mu_s = 0.30$ and $\mu_k = 0.25$. The interface forces on the upper block should be equal in magnitude and opposite in direction to the applied loads. F_y should ramp linearly from zero to a peak value of 10.0 at time t = 0.1 and then remain constant. The relative y-displacement between the two bodies should be zero for all time. The relative x-displacement should be zero until P_x exceeds the static friction force, $f_s = 3.0$, just before time t = 0.4. The upper block should then slide along the interface. F_x should be zero until t = 0.3 and then ramp linearly to a value of -3.0 near t = 0.4; it should then drop to the dynamic friction force, $f_k = -2.5$. R_x should be equal in magnitude and opposite in sign to F_x. The expected interface and reaction force time histories are given in Figure 3.

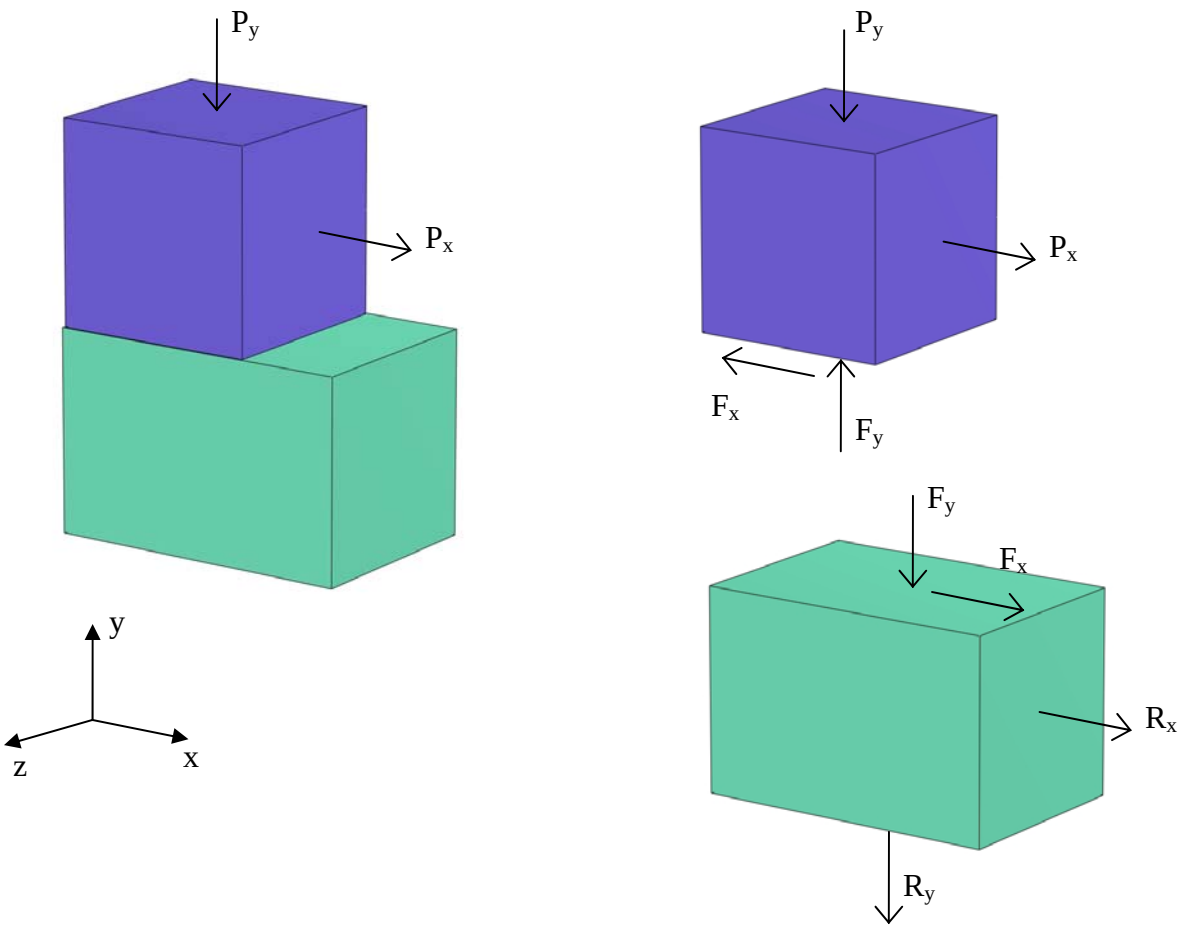

Figure 2. The two-body contact problem uses equilibrium considerations to determine the interface and reaction forces.

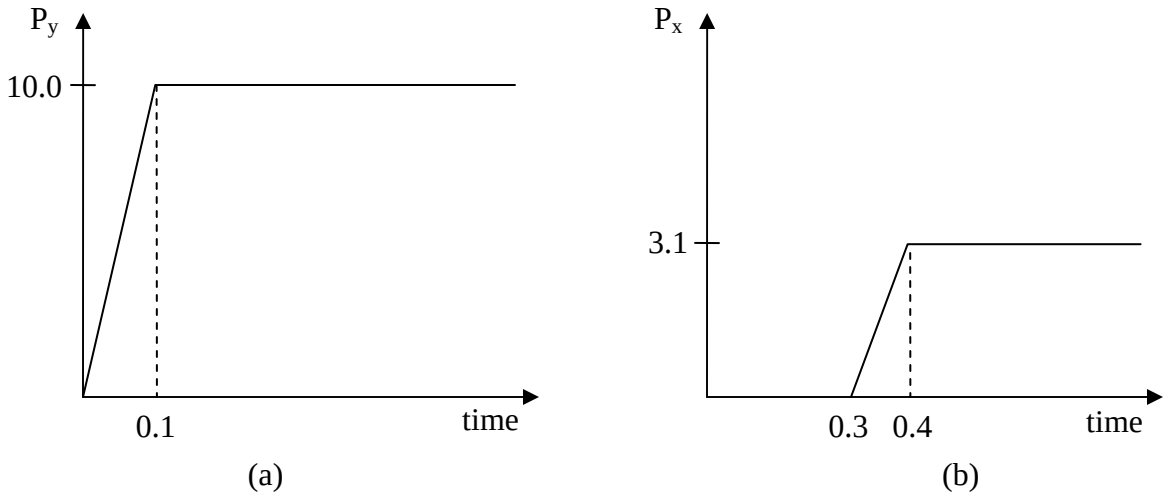

Figure 1. The loads for the two-body contact problem are applied first in the y-direction (a) and then in the x-direction.

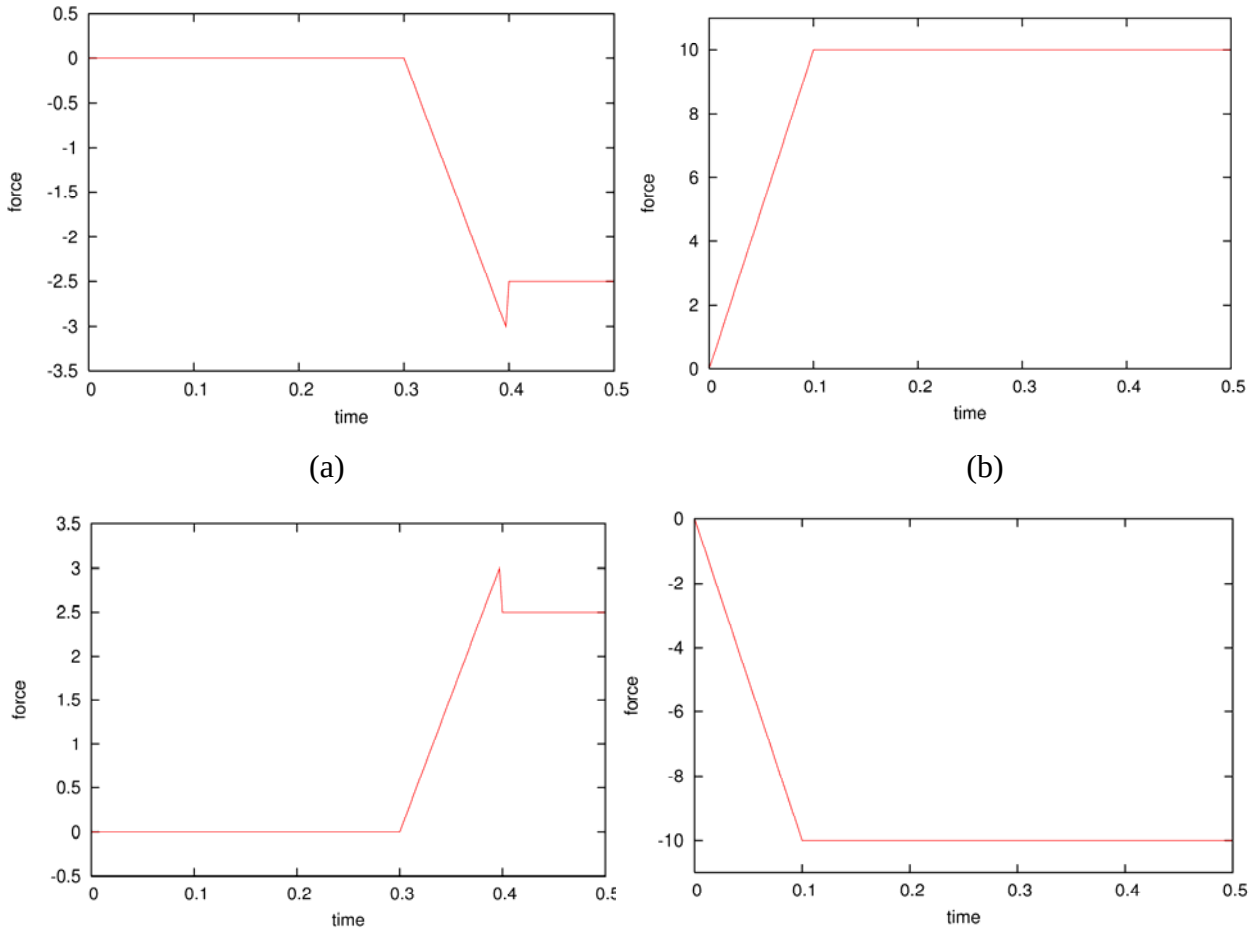

Figure 3. The expected force time histories F_x (a), F_y (b), R_x (c), and R_y (d) for the two-body contact problem.

2.2 THREE-BODY CONTACT PROBLEM

The three-body contact problem is depicted schematically in Figure 4. The interface behavior between the upper and middle blocks (upper interface) and the middle and lower blocks (lower interface) is idealized by a traditional Coulomb friction model. The upper and lower blocks are constrained in the x-direction along their right side (positive x-face). Additionally, the lower block is constrained along its bottom surface against movement in the y-direction. The upper and lower blocks are 1 unit x 1 unit x 1 unit, while the middle block is 4.5 units x 1 unit x 1.04 units. The middle block's larger dimensions ensure that the interfaces remain in full contact while reacting to the applied loads.

The vertical force on the upper block P_y is applied first to establish a normal force across both the upper and lower interfaces. The tangential force P_x is applied next. The normal interface force on the upper interface is F_y^U and on the lower interface it is F_y^L. The tangential interface forces are F_x^U on the upper interface and F_x^L on the lower interface. The reaction force in the x-

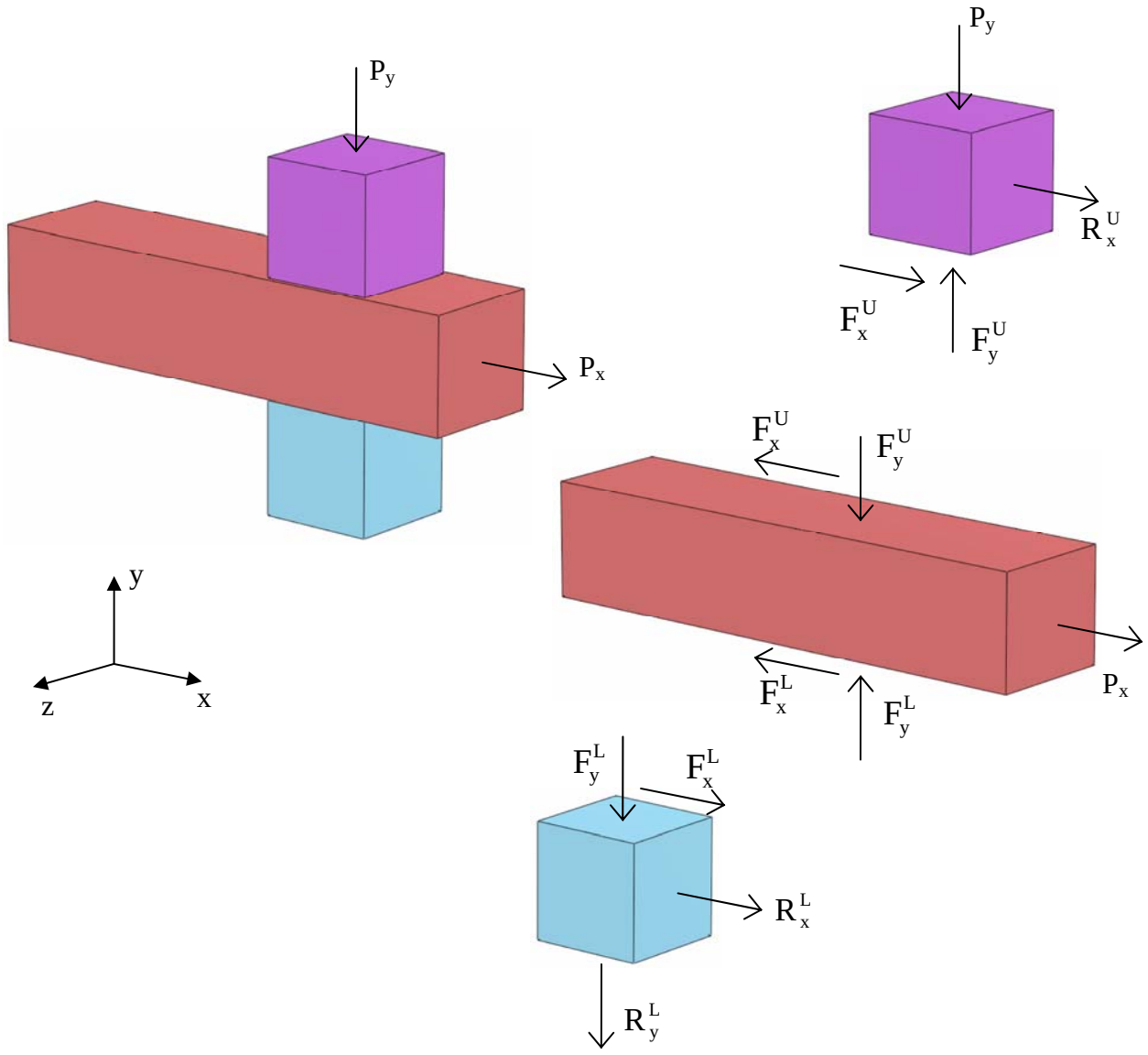

Figure 4. Equilibrium considerations are used to determine the interface and reaction forces for the three-body contact problem.

direction is R_x^U on the upper block and R_x^L on the lower block. The reaction force in the y-direction is R_y^L on the lower block. If the loads are applied slowly, then inertia effects can be ignored and a pseudo-static solution can be developed for the interface forces and reaction forces.

The z-direction interface force is zero since there is no applied load in the z-direction. Applying equilibrium to the upper block, F_y^U is equal in magnitude to P_y, but acts in the opposite direction. F_x^U is equal to R_x^U, where the reaction is defined as the force applied by the body against the constraint. On the middle block, F_y^L and F_y^U are equal and opposite, and the sum of the

tangential interface forces equals the applied tangential force, $F_x^U + F_x^L = P_x$. On the lower block, F_x^L equals R_x^L and F_y^L equals R_y^L. Therefore, the magnitude of the normal interface forces and normal reaction force is equal to the vertical applied load, $F_y^U = F_y^L = R_y^L = P_y$. Using symmetry arguments, F_x^U is equal to F_x^L and also equal to one-half the applied tangential load, $F_x^U = F_x^L = \frac{1}{2} P_x$, until the peak static friction force is reached. Then the magnitude of F_x^U and F_x^L is limited to the dynamic friction force.

2.2.1 Theoretical Solution for Three-Body Contact

Consider the pseudo-static response to the applied loads shown in Figure 5 when $\mu_s = 0.15$ and $\mu_k = 0.1375$. F_y^U on the upper block and F_y^L on the middle block should be equal in magnitude and opposite in direction to the applied load P_y. F_y^U and F_y^L should ramp linearly from zero to a peak value of 400.0 at time t = 0.2 and then remain constant. The relative y-displacement along both interfaces should be zero for all times. The relative x-displacement should be zero until P_x exceeds the total static friction force, $f_s = 2(\mu_s \text{ N}) = 120.0$, just before time t = 0.4. The middle block should then slide in the x-direction. F_x^U and F_x^L should be zero until t = 0.3 and then ramp linearly to a value of -60.0 near t = 0.4. After the peak friction force has been exceeded, the resistive force should drop to and remain at the total dynamic friction force, $f_k = 2(\mu_k \text{ N}) = 110.0$. The expected value of F_x^U and F_x^L during dynamic friction is -55.0. The reaction forces should be equal in magnitude and opposite in sign to the corresponding interface forces. The expected interface and reaction force time histories are given in Figure 6.

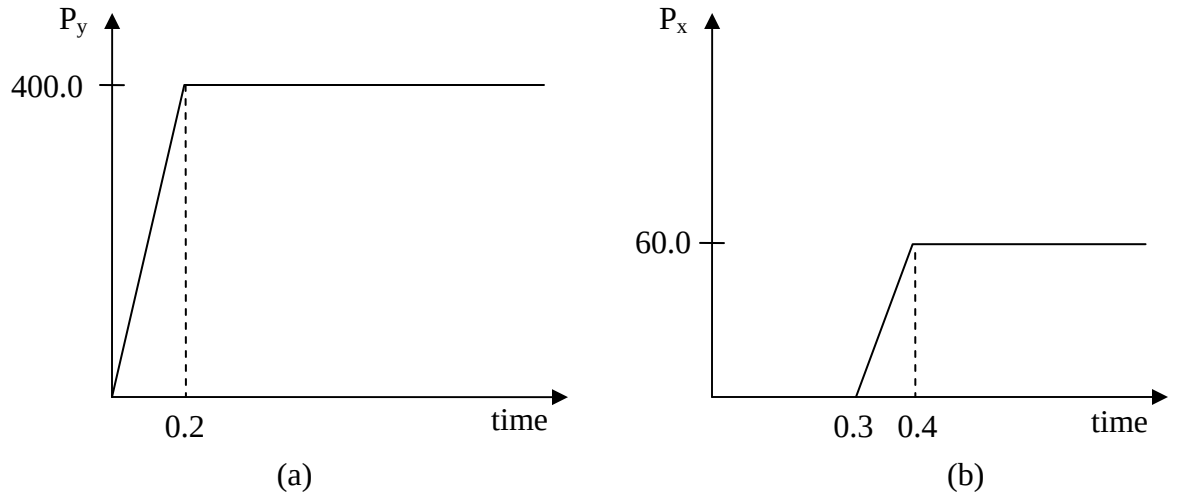

Figure 5. The loads for the three-body contact problem are applied first in the y-direction (a) and then in the x-direction (b).

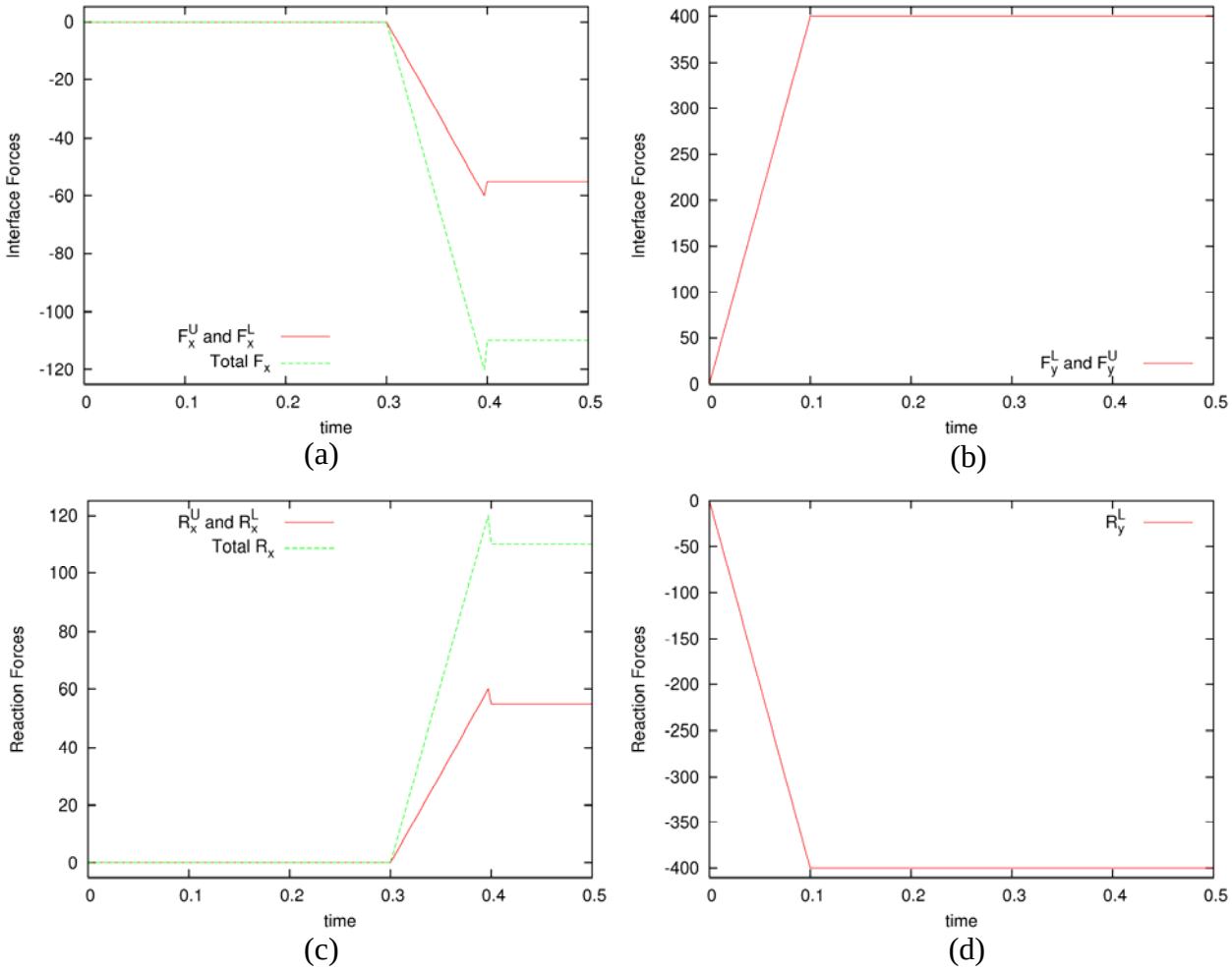

Figure 6. The expected force time histories F_x (a), F_y (b), R_x (c), and R_y (d) for the three-body contact problem.

3 FINITE ELEMENT REPRESENTATION

Many of the assumptions and approximations used to represent the test problems in the FEA model are discussed in the companion report (McMichael, 2006). Therefore, this section focuses on the implementation details for the current test problems and refers the interested reader to the companion report for a general description of the FEA modeling approach used.

3.1 TWO-BODY CONTACT PROBLEM

The two-body contact problem consists of four sets of upper and lower blocks. The finite element mesh is shown in Figure 7. The interfaces are represented using a mixture of Type 3 and Type 12 contact algorithms with penalty and Lagrange enforcement as given by Table 1. For the Type 3 interface, the slave surface is defined on the upper block and the master surface is on the lower block. Domain limitations are specified to limit the search regions for the automatic contact interfaces.

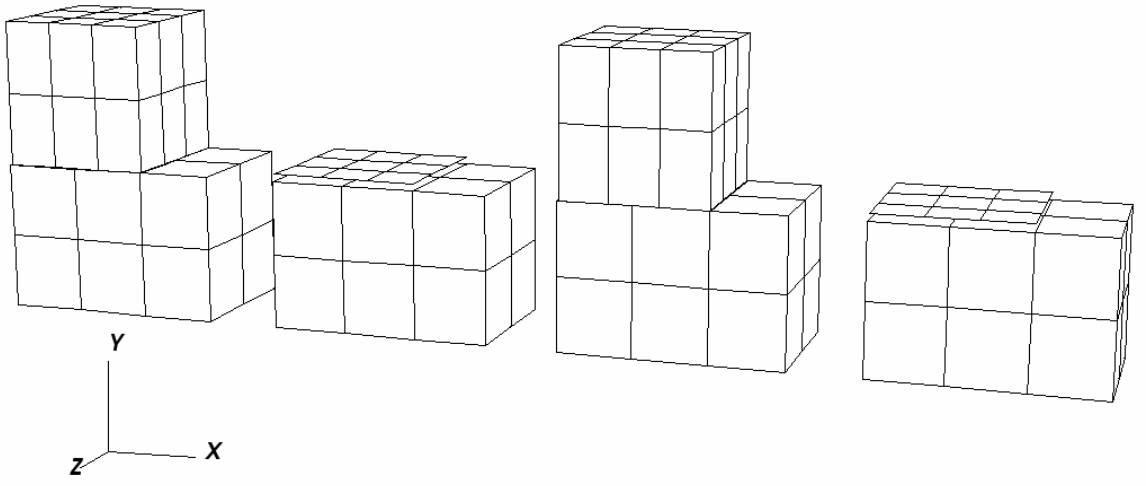

Figure 7. The finite element mesh used to represent the four body sets in the two-body contact problem.

Body Set	Interface Type	Enforcement Option
1	3	Penalty
2	3	Lagrange
3	12	Penalty
4	12	Lagrange

Table 1. A mixture of interface types and enforcement options are used in the two-body contact problem.

The upper block is a rigid material with the spatial domain represented using shells or solid elements. It has three elements in the x-direction and three elements in the z-direction. When solid elements (bricks) are used to represent the upper body, two elements are used in the y-direction. When shell elements are used for the upper block, the shell element thickness is 0.1. The shell material density is ten times larger than the solid material density to maintain a consistent mass for the upper block. The larger lower block is a deformable material with the spatial domain represented with solid elements. It has three elements in the x-direction, two elements in the y-direction, and two elements in the z-direction. Both contact algorithms account for the shell element thickness. The applied loads are imposed by body forces on the upper block.

The material response is idealized as linear elastic. The upper block is modeled using the rigid (Type 20) material model with an elastic modulus of 1000.0 and a Poisson ratio of 0.1. The lower block is modeled using the hyperelastic Mooney-Rivlin (Type 27) formulation and hourglass stabilization method 10. The material properties are given in Table 2. The selected

Mooney-Rivlin material properties result in an elastic modulus that is four times greater than the one selected for the rigid materials (which is used for calculating the interface segment stiffness). Frictional behavior in DYNA3D is represented using three coefficients. The coefficient of static friction, μ_s, the coefficient of kinetic friction, μ_k, and an exponential decay coefficient, β. The transition between static and dynamic friction is controlled by β and the relative velocity between the two (master and slave) surfaces. The friction coefficients used for all four interfaces are given in Table 3.

Mooney – Rivlin (Type 27)	
Density	0.01
First Invariant Coefficient, A	909.091
Second Invariant Coefficient, B	0.0
Poisson Ratio	0.1
Hourglass Stabilization Method	10
Quadratic Bulk Viscosity Coefficient	1.5
Linear Bulk Viscosity Coefficient	0.06

Table 2. Material properties used for the continuum elements.

Coefficient of Static Friction, μ_s	0.30
Coefficient of Kinetic Friction, μ_k	0.25
Exponential Decay Coefficient, β	2.0

Table 3. The friction coefficients used for the interfaces.

3.2 THREE-BODY CONTACT PROBLEM

The three-body contact problem uses four body sets as shown in Figure 8. The frictional interfaces are represented using the Type 3, 5, 10, and 12 contact algorithms. A third interface is introduced to each body set by representing the middle block as two halves joined in the middle by a tied interface. Both Type 2 (kinematic enforcement) and Type 9 (penalty enforcement) interfaces are used. The normal and shear failure stresses for the Type 9 interface are set to 10,000.0 to prevent relative movements due to interface failure. Therefore, the twelve interface definitions in the three-body contact problem are a mixture of six interface types and three enforcement options. The interface type and enforcement option used for each interface are listed in Table 4. Domain limitations are specified to limit the search regions for the automatic contact interfaces, and a penalty stiffness scale factor of 3.0 is used for all penalty enforcement algorithms.

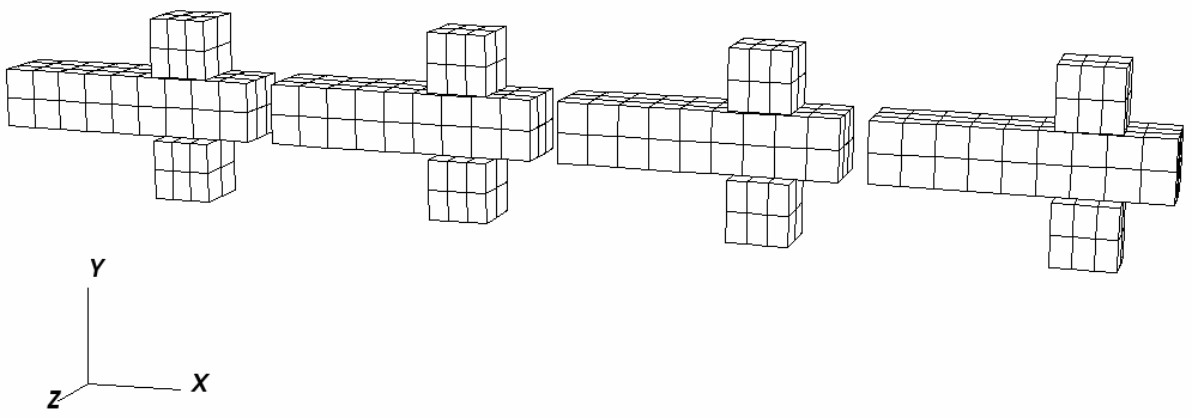

Figure 8. The finite element mesh used to represent the four body sets in the three-body contact problem.

Body Set	Upper Interface	Middle Interface	Lower Interface
1	10 Lagrange	9 Penalty	5 Penalty
2	5 Lagrange	2 Kinematic	12 Penalty
3	3 Lagrange	2 Kinematic	10 Penalty
4	12 Lagrange	9 Penalty	3 Penalty

Table 4. The interface type and enforcement option used for each interface in the three-body contact problem.

The upper block is represented using solid elements with three elements in the x-direction, two elements in the y-direction, and two elements in the z-direction. The middle block is also represented using solid elements. The top and bottom halves each have nine elements in the x-direction, one element in the y-direction, and three elements in the z-direction. The lower block's spatial domain is represented using a combination of shell and solid elements with a layer of shell elements bonded to the top surface of the lower block. There are three elements in the x-direction and two elements in the z-direction for both element types, and two elements in the y-direction for the solids. The shell material density is five times larger than the solid material density. The shell element thickness is 0.2 and is accounted for by all of the contact algorithms. The applied loads are imposed by vertical body forces on the upper block and horizontal body forces on the middle block.

The material response is idealized as linear elastic. The solid elements are modeled using the hyperelastic Mooney-Rivlin (Type 27) formulation and hourglass stabilization method 10. The shells are represented using the linear elastic (Type 1) material model with hourglass stabilization method 2. The material properties were chosen for numerical convenience and are given in Table 5. The selected Mooney-Rivlin material properties result in an elastic modulus that is ten times greater than the one selected for the shells. Frictional behavior in DYNA3D is represented using three coefficients. The coefficient of static friction, μ_s, the coefficient of kinetic friction, μ_k, and an exponential decay coefficient, β. The transition between static and

dynamic friction is controlled by β and the relative velocity between the two (master and slave) surfaces. The coefficients used for all frictional interfaces are given in Table 6.

Continuum Elements Material Properties: Mooney – Rivlin (Type 27)	
Density	0.01
First Invariant Coefficient, A	1.136E+05
Second Invariant Coefficient, B	0.0
Poisson Ratio	0.1
Hourglass Stabilization Method	10
Quadratic Bulk Viscosity Coefficient	1.5
Linear Bulk Viscosity Coefficient	0.06

Shell Elements Material Properties: Linear Elastic (Type 1)	
Density	0.05
Elastic Modulus	50,000.0
Poisson Ratio	0.1
Element Formulation	2
Shell Thickness	0.2
Number of Through Thickness Gauss Integration Points	5
Hourglass Stabilization Method	2
Hourglass Stabilization Coefficient	0.1
Quadratic Bulk Viscosity Coefficient	1.5
Linear Bulk Viscosity Coefficient	0.06

Table 5. Material properties used for the three-body contact problem.

Coefficient of Static Friction, μ_s	0.15
Coefficient of Kinetic Friction, μ_k	0.1375
Exponential Decay Coefficient, β	1.8

Table 6. The friction coefficients used for the three-body contact problem.

4 EXPECTED RESULTS

The expected results for the two-body and three-body contact problems are discussed with respect to four verification criteria: 1) observed deformations, 2) relative nodal displacements, 3) interface forces, and 4) reaction forces. The observed deformations are a gross qualitative check on the interface behavior to ensure that the nodal displacements conform to the kinematic restrictions the contact algorithms are supposed to enforce. Relative nodal displacements measure changes in the distance separating the master and slave surfaces and provide a quantitative check on the kinematic restrictions. The magnitude and direction of the total interface forces output by DYNA3D are compared to the theoretical static solutions developed in sections 2.1.1 and 2.2.1. The reaction forces associated with prescribed boundary conditions provide an indirect, quantitative measure of the interface forces.

4.1 EXPECTED TWO-BODY CONTACT RESULTS

The two-body contact problem's deformations should exhibit no apparent interpenetration along the interface, and the upper block should slide only in the x-direction. The relative y-displacement between the slave and master surfaces should be zero for all time. The relative x-

displacement should be zero until the body force in the x-direction exceeds f_s = 3.0, just before time t = 0.4. Time history results are generated for each interface using the slave and master surface nodal pairs given in Table 7. The interface nodes are selected such that their initial position is close to the center of the contact area between the blocks. The slave surface interface forces F_x and F_y should correspond to the theoretical solutions shown in Figure 3 (a) and (b), respectively. The reaction forces R_x and R_y should be equal in magnitude and opposite in sign to the interface forces and should correspond the theoretical solutions shown in Figure 3 (c) and (d), respectively.

	Body Set 1	Body Set 2	Body Set 3	Body Set 4
Slave Node	14	90	150	226
Master Node	77	129	213	265

Table 7. The slave and master surface nodal pairs used to generate relative displacement time histories for each interface in the two-body contact problem.

4.2 EXPECTED THREE-BODY CONTACT RESULTS

Deformations in the three-body contact problem should reveal no apparent interpenetration along the interfaces, the two halves of the middle block should maintain their relative nodal positions, and relative motion should only occur in the x-direction when the middle block slides. The relative y-displacement between the slave and master surfaces should be zero for all interfaces and all times. The relative x-displacement for the upper and lower interface should be zero until just before time t = 0.4 when the body force in the x-direction exceeds f_s = 120.0. Time history results are generated for each interface using the slave and master surface nodal pairs given in Table 8. The interface nodes are selected such that their initial position is close to the center of the contact area between the blocks.

		Body Set 1	Body Set 2	Body Set 3	Body Set 4
Upper Interface	Slave Node	11	243	475	707
	Master Node	91	323	555	787
Middle Interface	Slave Node	163	395	627	859
	Master Node	79	311	543	775
Lower Interface	Slave Node	201	433	665	897
	Master Node	166	398	630	862

Table 8. The slave and master surface nodal pairs used to generate relative displacement time histories for each interface in the three-body contact problem.

The interface x-forces acting on the middle block, F_x^U and F_x^L, and the total interface x-force F_x should correspond to the theoretical solutions shown in Figure 6 (a). The interface y-force from the upper block F_y^U, the interface y-force from the middle block F_y^L, and the total interface y-force F_y should correspond to the theoretical solutions shown in Figure 6 (b). The reaction forces in the x-direction, R_x^U and R_x^L, and the total reaction force in the x-direction R_x should be equal and opposite to the corresponding interface forces and should correspond the theoretical

solutions shown in Figure 6 (c). The reaction force in the y-direction, R_y^L, should be equal and opposite to F_y^L and should correspond to the theoretical solution shown in Figure 6 (d).

On the middle interface, the interface x-force should be zero due to symmetry. The vertical applied force should be transferred through the middle block. Therefore, the interface y-force acting on the upper half of the middle block should correspond to the theoretical solution shown in Figure 6 (b).

4.3 FACTORS INFLUENCING THE NUMERICAL RESULTS

As discussed in the basic contact report, the DYNA3D results include transient dynamic effects that are not present in the static solution. The numerical results are expected to show some oscillations that should decay over time and converge to the static solution. It is also expected that the exponential friction law implemented in DYNA3D will produce a more rounded transition from static to dynamic friction than then instantaneous theoretical transition. Peak displacements and peak forces may also be underrepresented in the numerical results since values are output at a specified interval and the peak may occur between output states.

The total interface force is a good quantitative measure for most contact algorithms, but not for automatic contact (Type 12). This is because automatic contact treats all interface segments as master segments and all nodes as slave nodes. As a result, the total interface force for automatic contact with penalty enforcement is always zero. When automatic contact is used with the Lagrange enforcement method, the total interface force represents the sum of the restoration forces applied to all slave nodes. However, some force cancellation may occur since segments may be oriented in opposite directions. Thus, for automatic contact, the total force reported by DYNA3D is typically lower than the actual force and is not a reliable measure. Since static equilibrium considerations require the reaction forces to balance the interface forces and applied loads on each block, the reaction forces are able to quantify the interface forces by indirect means.

5 NUMERICAL RESULTS

5.1 TWO-BODY CONTACT RESULTS

The mesh exhibits the expected deformation as the body forces are applied. The relative normal displacements are shown in Figure 9. Interpenetrations are well controlled in all the body sets, with peak magnitudes on the order of 3.0E-04 for the shell-on-solid problems (Body Sets 2 and 4) and 8.5E-03 for the solid-on-solid problems (Body Sets 1 and 3). The interface forces developed by the Type 3 surfaces are shown in Figure 10 and correspond very well with the expected time history. The peak friction force is under predicted by both enforcement methods. The peak interface force reported by the penalty enforcement method is 2.89 (96% of theoretical) compared to 2.71 (90% of theoretical) for the Lagrange enforcement method. The interface force during dynamic friction matches expectations very well for both enforcement methods. The reaction forces (Figure 11) indicate that the Type 12, automatic contact algorithms also perform well. The Type 12 interface results closely match those for the Type 3 interface. Overall, the two-body contact problem demonstrates very good correlation with the theoretical solution for both interface types, both enforcement methods, and both element interactions (shell-on-solid

and solid-on-solid). There are no apparent interface logic problems or interaction problems between rigid and deformable bodies.

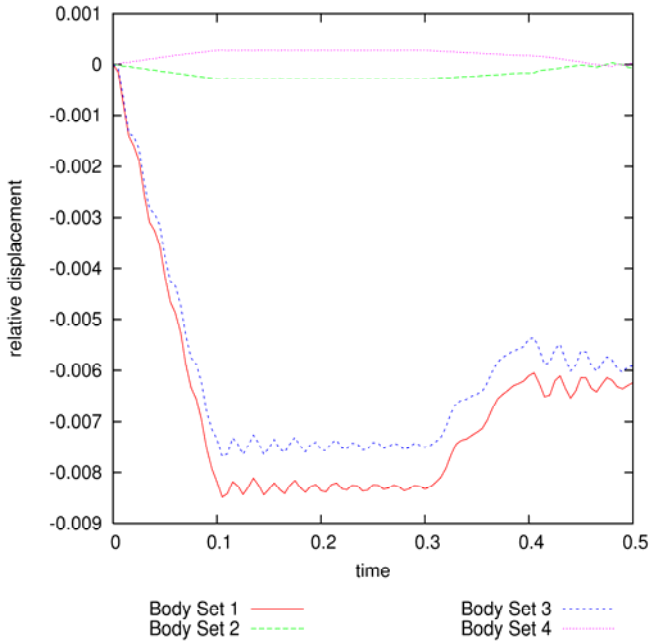

Figure 9. The relative y-displacements show only minor interpenetration in the two-body contact problem.

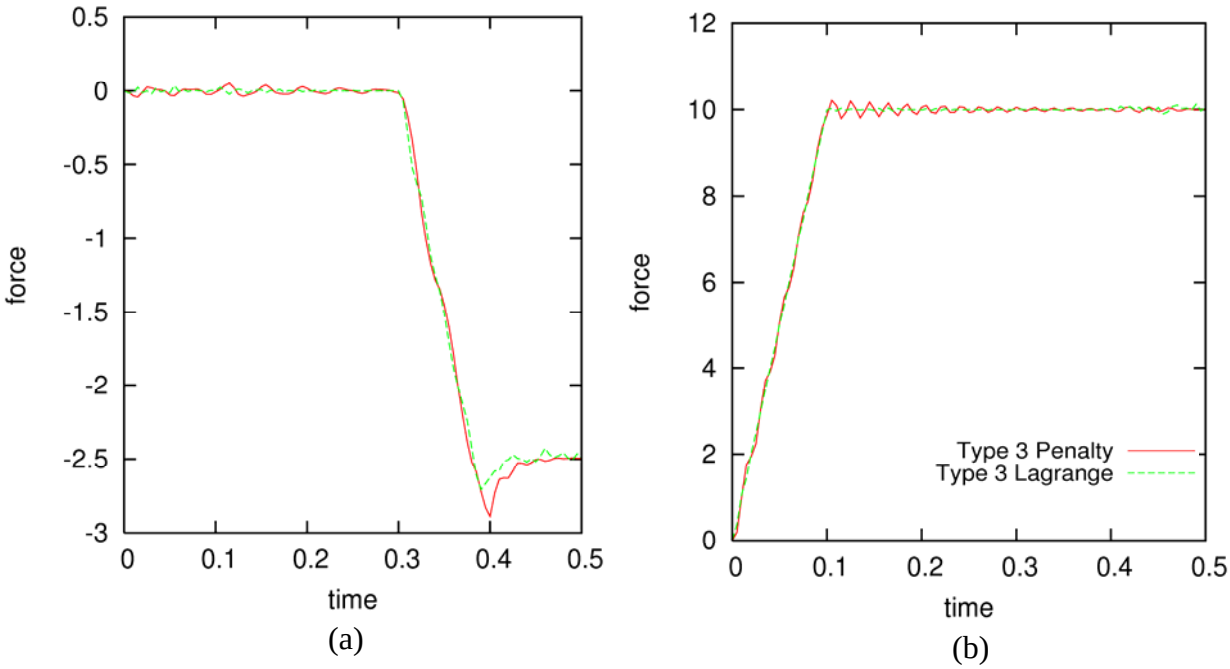

Figure 10. The interface force time histories F_x (a) and F_y (b) for the non-automatic contact interfaces in the two-body contact problem. The expected peak magnitudes are F_x = -3.0 and F_y = 10.0.

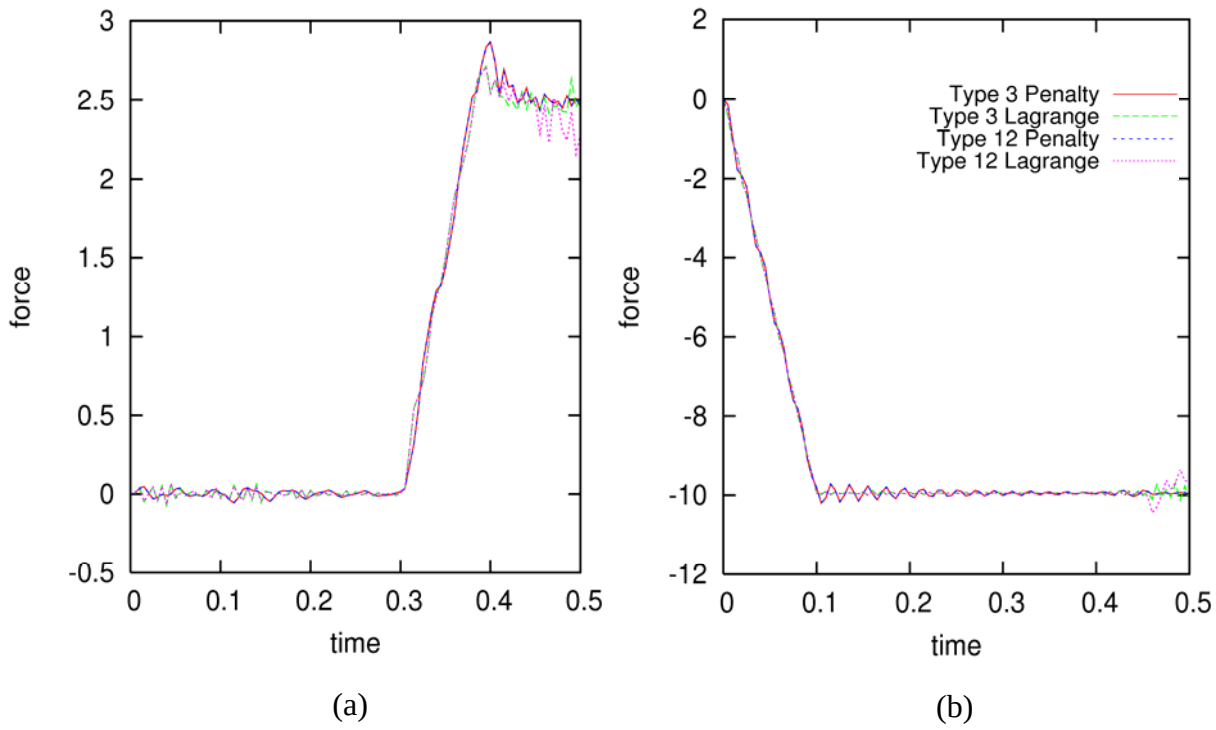

Figure 11. The reaction force time histories R_x (a) and R_y (b) for the two-body contact problem. The expected peak magnitudes are R_x = 3.0 and R_y = -10.0

5.2 THREE-BODY CONTACT RESULTS

The observed deformations correspond very well to expectations as the body forces are applied. The relative normal displacements (Figure 12) follow a pattern. For all four body sets, the lower interface's penalty enforcement limits interpenetrations to approximately 1.8E-03. The upper interface's Lagrange enforcement restricts interpenetrations to approximately 1.5E-04, an order of magnitude less than the penalty enforcement interpenetrations. The interpenetration along the middle interface shows some variation depending upon the contact enforcement method. Kinematic enforcement (Type 2) allows no interpenetration, while penalty enforcement (Type 9) allows small interpenetrations on the order of 1.0E-03.

The interface forces and reaction forces developed in Body Set 1 through Body 4 are shown in Figure 13 through Figure 16, respectively. The interface forces for the automatic contact (Type 12) interfaces are not included in the figures. There are some minor asymmetries in the response that differ from the theoretical solution. For example, consider the interface forces for Body Set 1 shown in Figure 13. The lower interface (Type 5, penalty enforcement) reaches the peak static friction force before the upper interface (Type 10, Lagrange enforcement) does. However, the total interface force F_x matches the theoretical solution very well. Some transient dynamic effects are apparent in the results as well. For example, consider the interface forces and reaction forces for Body Set 4 shown in Figure 16. Both F_x and R_x experience significant oscillations as the vertical body force is applied. These oscillations last for approximately half of the vertical load application interval before settling to the expected zero value until t = 0.3. One possible explanation for these initial oscillations is "chatter" in the upper interface. Small variations in the

interpenetrations allowed by the penalty enforcement method used for the Type 9, middle interface could produce a slight rocking in the bodies. The Lagrange enforcement algorithm used for the Type 12, upper interface could be sensitive to the rocking motion while the interface normal force is relatively small. After the interface normal force is well established, the chatter would be suppressed. Smaller oscillations are apparent in the results for the other body sets; however, these oscillations tend to decay quickly to the expected static solution values.

Overall, the interface behavior matches the static solution very well. Interpenetrations are controlled, and the interface forces capture the peak static friction force before transitioning to dynamic friction. The reaction forces further support the conclusion that forces are appropriately transferred across the contact interfaces. There are no apparent interface logic problems due to the mixture of interface types, the multiple instances of each interface type, or the combination of enforcement methods.

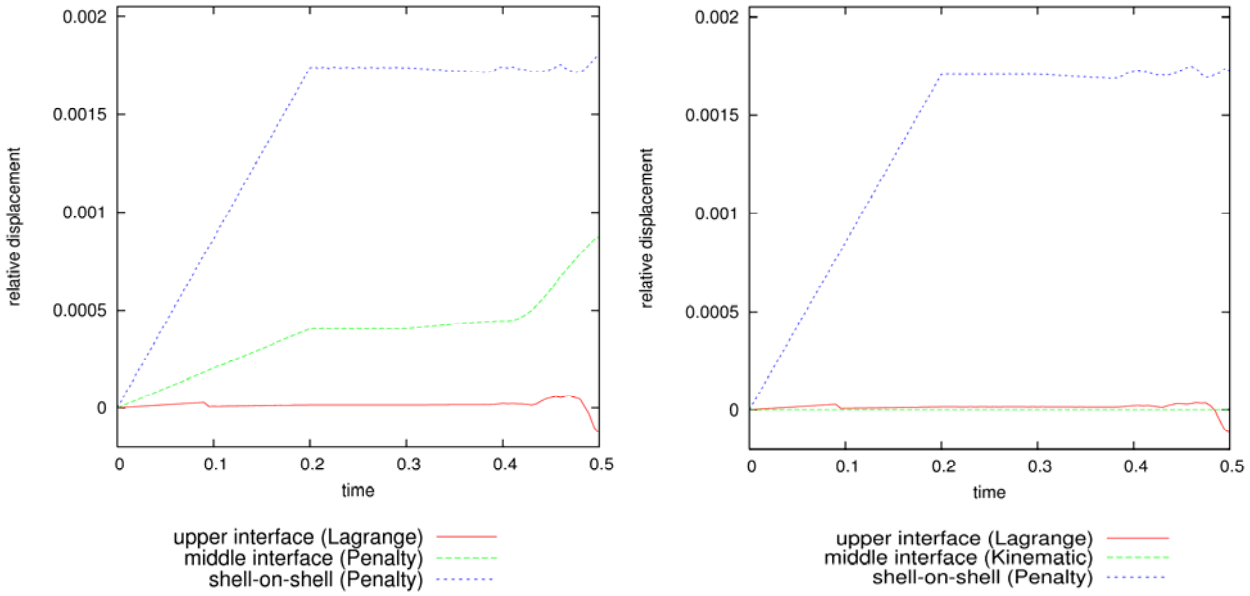

Figure 12. Typical relative y-displacements for the three-body contact problem show more interpenetration occurs along the middle interface when a penalty enforcement method is used (a) relative to a kinematic method (b).

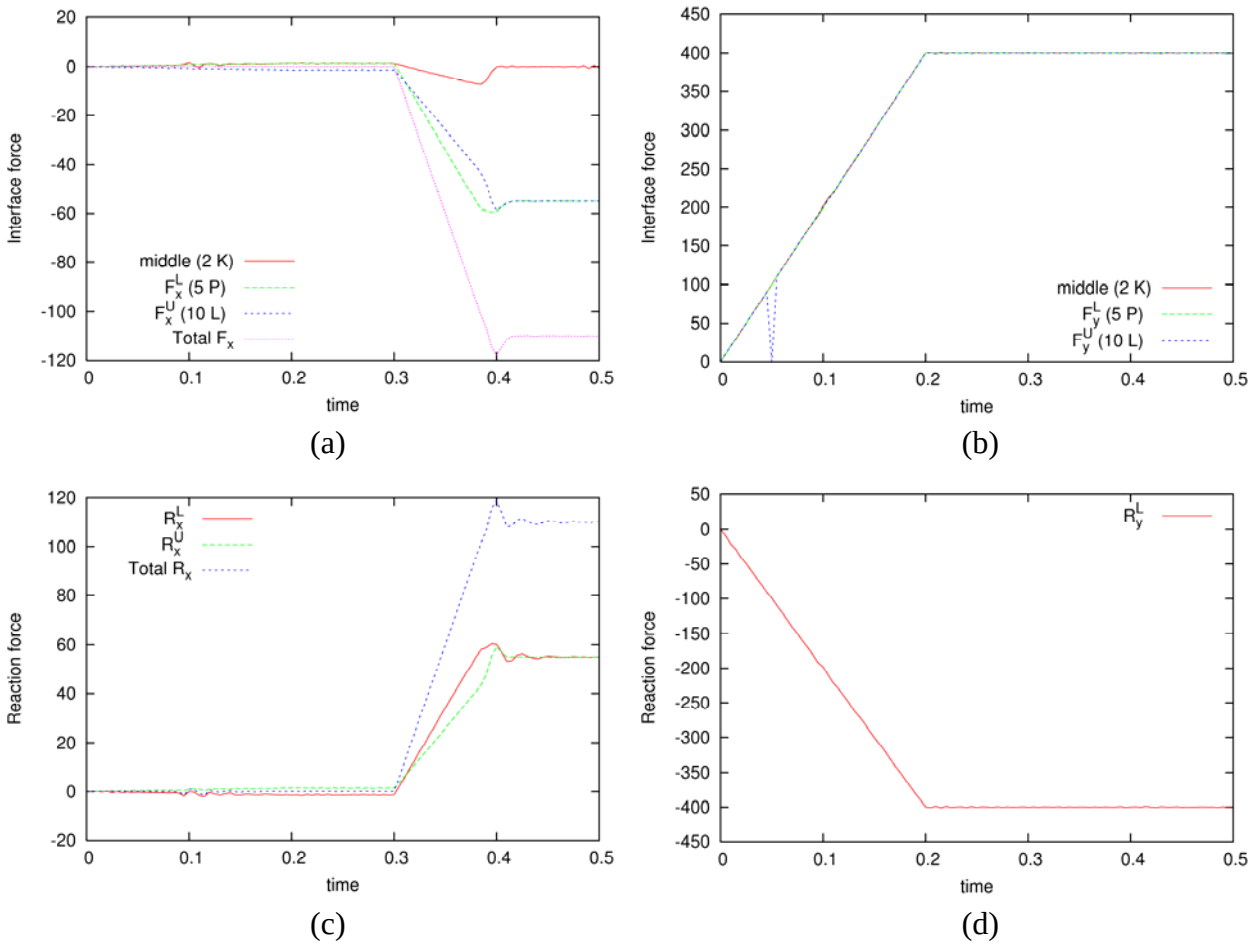

Figure 13. The interface forces, F_x (a) and F_y (b), and the reaction forces, R_x (c) and R_y (d), for Body Set 1 in the three-body contact problem. The expected peak magnitudes are: $F_x^U = F_x^L = -60.0$, $F_x = -120.0$, $F_y^U = F_y^L = 400.0$, $R_x^U = R_x^L = 60.0$, $R_x = 120.0$, and $R_y = 400.0$.

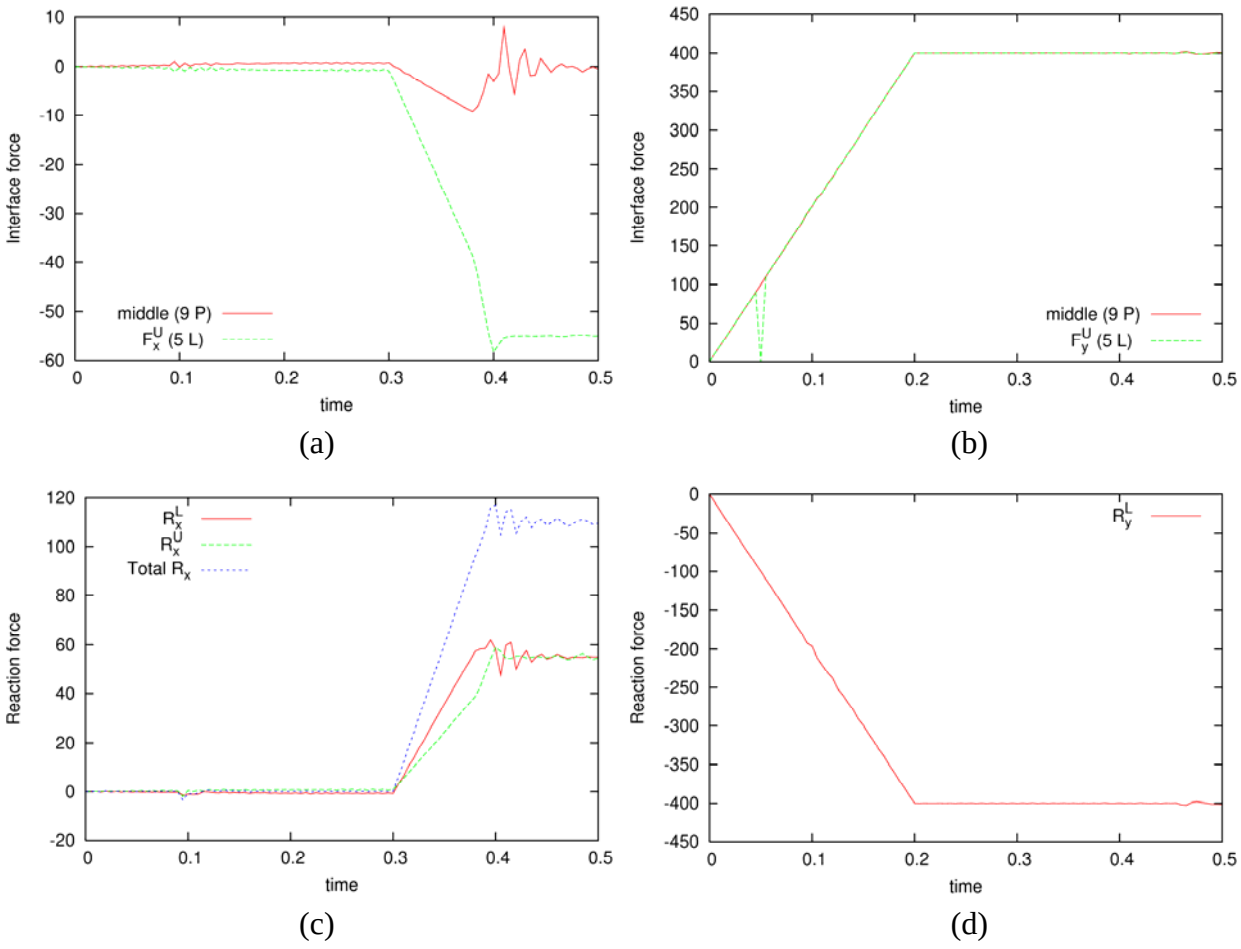

Figure 14. The interface forces, F_x (a) and F_y (b), and the reaction forces, R_x (c) and R_y (d), for Body Set 2 in the three-body contact problem. The expected peak magnitudes are: $F_x^U = F_x^L = -60.0$, $F_x = -120.0$, $F_y^U = F_y^L = 400.0$, $R_x^U = R_x^L = 60.0$, $R_x = 120.0$, and $R_y = 400.0$.

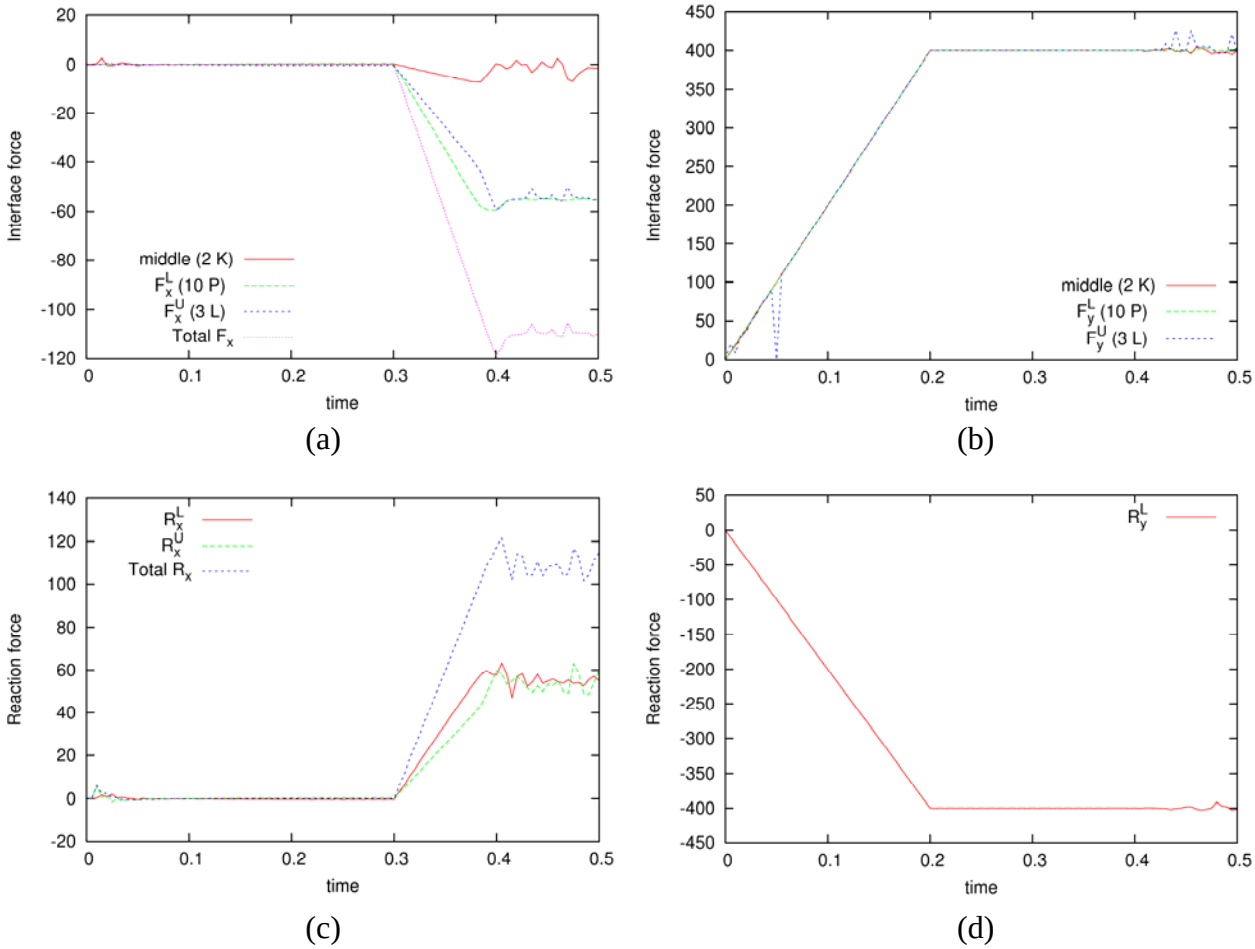

Figure 15. The interface forces, F_x (a) and F_y (b), and the reaction forces, R_x (c) and R_y (d), for Body Set 3 in the three-body contact problem. The expected peak magnitudes are: $F_x^U = F_x^L = -60.0$, $F_x = -120.0$, $F_y^U = F_y^L = 400.0$, $R_x^U = R_x^L = 60.0$, $R_x = 120.0$, and $R_y = 400.0$.

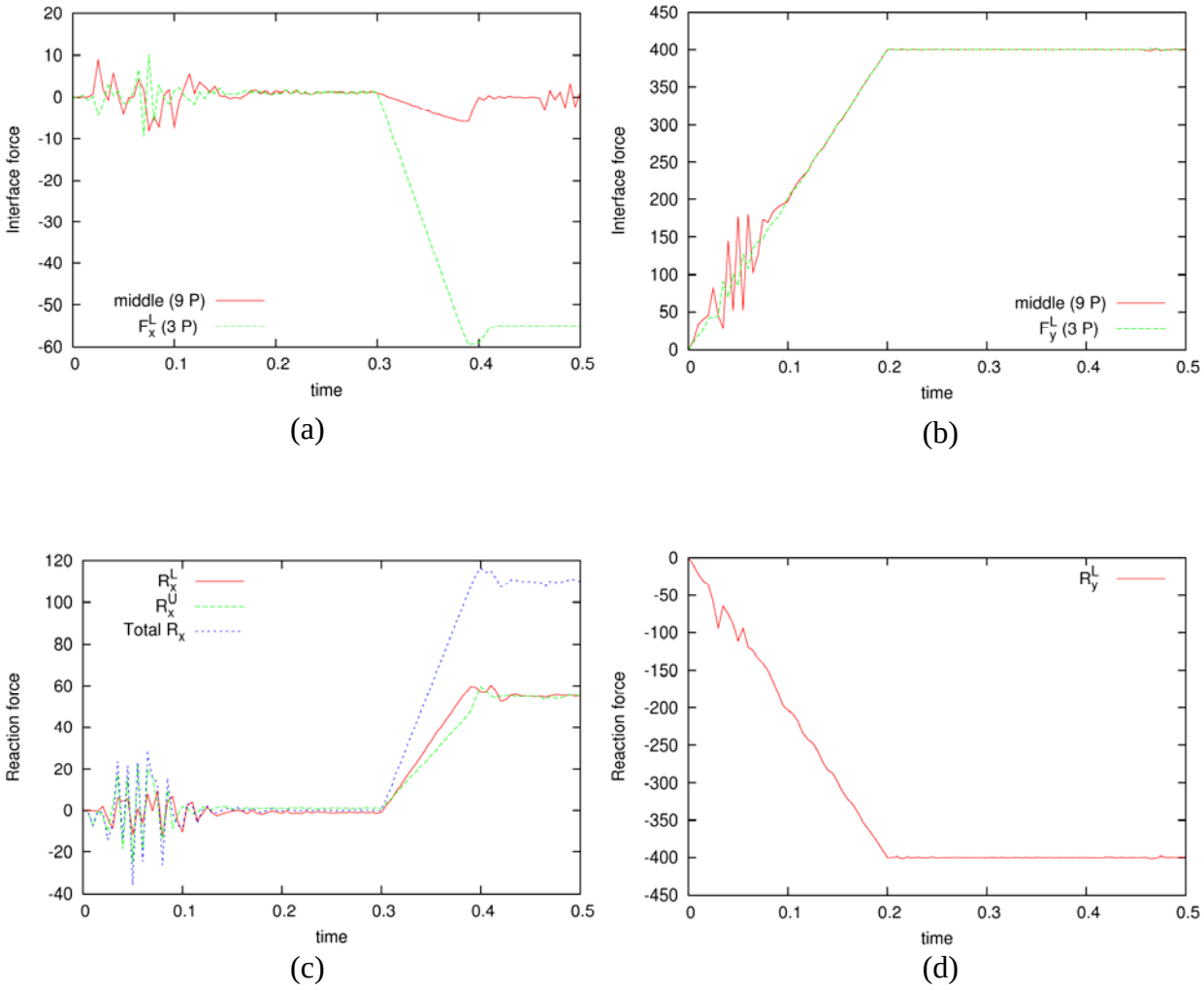

Figure 16. The interface forces, F_x (a) and F_y (b), and the reaction forces, R_x (c) and R_y (d), for Body Set 4 in the three-body contact problem. The expected peak magnitudes are: $F_x^U = F_x^L = -60.0$, $F_x = -120.0$, $F_y^U = F_y^L = 400.0$, $R_x^U = R_x^L = 60.0$, $R_x = 120.0$, and $R_y = 400.0$.

6 SUMMARY OF INTERFACE BEHAVIOR

The multi-contact test suite demonstrates the versatility and capabilities of the DYNA3D contact algorithms to capture the interaction between multiple interfaces. Interface behavior is evaluated with respect to observed deformations, nodal time histories, interface forces, and reaction forces. As anticipated, the exponential friction law in DYNA3D produces a more rounded transition from static to dynamic friction than the sharp, theoretical step-function, and the results include decaying oscillations due to the transient dynamics capabilities embedded in the DYNA3D analysis. Overall, the contact algorithms do a very good job representing the interface behavior. Observed mesh deformations closely match expectations, and relative displacements confirm that interpenetrations are limited to reasonable amounts. Normal and tangential forces are resolved very well for the interfaces, and the reaction forces demonstrate that the interfaces transfer the appropriate forces between bodies. The test problems provide no indication that the combination of interface types, the multiple instances of each interface type, the mixture of enforcement methods, or the interaction between rigid and deformable bodies produces any interface logic or ordering errors.

REFERENCES

1. Lin, J. I., "DYNA3D: A Nonlinear, Explicit Three-Dimensional Finite Element Code for Solid and Structural Mechanics, User Manual," University of California Lawrence Livermore National Laboratory, UCRL-MA-107254, **2005**.
2. McMichael, L. D., "Contact Interface Verification for DYNA3D, Scenario 1: Basic Contact," University of California Lawrence Livermore National Laboratory, UCRL-TR-221283, **2006**.

APPENDIX A: TEST PROBLEMS

File Name	Problem Description
sslideriqid.dyn	Serial verification problem for two-body contact between rigid and deformable bodies. The problem uses a mixture of Type 3 and Type 12 interfaces with penalty and Lagrange enforcement algorithms.
sslidemulti.dyn	Serial, multi-contact verification problem for three-body contact. Six interface types and three enforcement options are mixed to define the behavior along the twelve interfaces.